arXiv:1512.08194v2 [cs.DC] 12 Apr 2016

Executing Dynamic and Heterogeneous Workloads on Super Computers

Andre Merzky, Mark Santcroos, Matteo Turilli, Shantenu Jha
RADICAL Laboratory, Electric and Computer Engineering, Rutgers University, New Brunswick, NJ, USA

***Abstract*—Many scientific applications have workloads comprised of multiple heterogeneous tasks that are not known in advance and may vary in the resources needed during execution. However, high-performance computing systems are designed to support applications comprised of mostly monolithic, single-job workloads. Pilot systems decouple workload specification, resource selection, and task execution via job placeholders and late-binding. Pilot systems help to satisfy the resource requirements of workloads comprised of multiple tasks with the capabilities and usage policies of HPC systems. RADICAL-Pilot (RP) is a portable, modular and extensible Python-based Pilot system. In this paper we describe RP's design, discuss how it is engineered, characterize its performance and show its ability to execute heterogeneous and dynamic workloads on a range of high-performance computing systems. RP is capable of spawning more than 100 tasks/second and the steady-state execution of up to 8,000 concurrent tasks. RP can be used stand-alone, as well as integrated with other application-level tools as a runtime system.**

I. Introduction

Supercomputers have been designed to support applications comprised of mostly monolithic, single-job workloads. However, many important scientific applications have workloads comprised of multiple heterogeneous tasks that are not known in advance and may have dynamic relationships between tasks [1–3]. This requires middleware that can efficiently manage dynamic workloads and resources. In contrast, HPC systems have been designed and operated to maximize overall system utilization, which typically entails static resource partitioning across jobs and users. Thus, there is a tension between the resource requirements of *non-traditional* workloads and the capabilities of the traditional HPC system software as well as their usage policies.

Applications with workloads comprised of multiple tasks account for a relevant fraction of utilization [4, 5], are likely to grow in importance [6–8], and could benefit from better execution and resource management on HPC resources [9]. Consequently, the ability to support the resource requirements of these workloads without compromising traditional capabilities needs careful software ecosystem design.

Pilot systems have proven particularly effective in the execution of workloads comprised of multiple tasks on physically distributed resources. They decouple workload specification, resource selection, and task execution via job placeholders and late-binding. Pilot systems submit job placeholders (i.e., pilots) to the scheduler of resources. Once active, each pilot accepts and executes tasks directly submitted to it by the application (i.e., late-binding). Tasks are thus executed within time and space boundaries set by the resource scheduler, yet are scheduled by the application.

Pilot systems address two apparently contradictory requirements: accessing HPC resources via their centralized schedulers while letting applications independently schedule tasks on the acquired portion of resources. By implementing multi-level scheduling and late-binding, Pilot systems not only lower task scheduling overhead, mitigate queuing delays, and enable higher task execution throughput, but they also enable greater control over the resources acquired to execute heterogeneous and dynamic workloads. As such, Pilot systems provide a promising starting point to ease the tension between the resource requirements of workloads comprised of heterogeneous and dynamic tasks and the the capabilities of the traditional HPC system software.

Due to socio-technical reasons, the development of Pilot systems has been mainly tailored to specific user communities or resources [10] and relegated to distributed computing. This has limited the appreciation of the generality of the "Pilot abstraction" [10, 11]. In turn, this has resulted in implementations of Pilot systems that do not exploit the full potential of the Pilot abstraction to support the execution of workloads comprised of multiple tasks.

In this paper, we introduce and experimentally characterize RADICAL-Pilot (RP), a Pilot system that fully implements the concepts and capabilities of the Pilot abstraction. Accordingly, the design of RP imposes no constraints on the heterogeneity and dynamism of both workload and resources. RP supports heterogeneity by concurrently executing tasks with different properties and couplings on resources with diverse architecture and software environments. Dynamism is supported by managing the runtime variations of the number, properties and coupling between tasks.

The implementation of RP differs from other Pilot systems mostly in terms of API, portability, and introspection. Implemented in Python, RP is a self-contained Pilot system which can be used to provide a runtime system for applications with heterogeneous and dynamic workloads. RP exposes an application-facing API called "Pilot API" [12] and utilizes SAGA [13] to interface to the resource layer. RP provides method-level profiling for each RP module which enables a precise and fine-grained measurement of the overheads. RP can provide runtime capabilities when interfaced with other application-level tools [14, 15], workflow and workload management systems such as Swift [16] and PanDA [17]

respectively. However, RP is not a workflow system and does not provide workload management capabilities itself.

In Section II, we provide a summary of related work describing the distinctive capabilities of RP with respect to existing systems. Section III discusses the design and architecture of RP, establishing how it is a faithful implementation of the Pilot Abstraction engineered for scale and functionality. Section IV provides the results of the core experiments of this paper and an analysis of the results.

II. Related Work

Since 1995, around twenty systems with pilot capabilities have been implemented [10]. Some noteworthy highlights are presented: AppLeS [18] offered one of the first implementation of resource placeholders and application-level scheduling; HTCondor [19] and Glidein [20] enabled pilot-based concurrent execution on multiple and diverse resources; and DIANE [21], AliEn [22], DIRAC [23], PanDA [17], and GlideinWMS [24] brought pilot-based workload executions to the LHC communities.

In contrast to RP, these systems are tailored for specific workloads, resources, interfaces, or development models. They often encapsulate pilot capabilities within monolithic tools with greater functional scope. HTCondor with Glidein on OSG [25] is one of the most widely used Pilot systems but serves mostly single core workloads. The Pilot systems developed for the LHC communities execute millions of jobs a week [17] but specialize on supporting LHC workloads and, in most cases, specific resources like those of WLCG.

Similar specialization can be found in systems without pilot capabilities. For example, CRAM [26] is a tool developed to execute static ensembles of MPI tasks on HPC resources, one of the workload types also supported by RP. Developed for Sequoia, an IBM BG/Q system at LLNL, CRAM parallelizes the execution of an application with many input parameters by bundling it into a single MPI executable. Compared to CRAM, RP generalizes ensemble capabilities for both MPI and non-MPI applications, and for applications for which execution plans are not known in advance. In addition to IBM BG/Q, RP also provides these generalized capabilities on many other HPC systems.

Recognizing the potential for High-Throughput Computing (HTC) on HPC resources, IBM developed an HTC mode resembling a Pilot system [27] for the series of IBM BG/L products. Unsupported by later IBM Blue Gene series, RP brings back this HTC capability generalizing it to HPC architectures beyond IBM BG/L machines.

Pilots and pilot-like capabilities are also implemented by various workflow management systems. Pegasus [28] uses Glidein via providers like Corral [29]; Makeflow [30] and FireWorks [31] enable users to manually start workers on HPC resources via master/worker tools called Work Queue [32] and LaunchPad [31]; and Swift [16] uses two Pilot systems called Falkon [33] and Coasters [34]. In these systems, the pilot is not always a stand-alone capability and in those cases any innovations and advances of the pilot capability are thus confined to the encasing system.

Pegasus-MPI-Cluster (PMC) [35] is an MPI-based Master/Worker framework that can be used in combination with Pegasus. In the same spirit as RP, this enables Pegasus to run large-scale workflows of small tasks on HPC resources. In constrast with RP, tasks are limited to single node execution. In addition there is a dependency on $fork()/exec()$ on the compute node which rules out PMC on some HPC resources.

Falkon is an early example of a Pilot system for HPC environments. Similar to RP, Falkon exposes an API that is used to develop distributed applications or to be integrated within an end-to-end system such as with Swift. Different to RP, Falkon is optimized for single core applications. Consistent with RP, it has been designed to implement concurrency at multiple levels including dispatching, scheduling, and spawning of tasks across multiple compute nodes of possibly multiple resources.

Coasters is similar to RP in that it supports heterogeneity at resource level. RP supports a greater variety of resources though, mainly due to the use of SAGA as its resource interoperability layer. The two systems differ in their architectures and workload heterogeneity (RP also supports multi-node MPI applications).

JETS [36] is a middleware component providing Swift and Coasters with high performance support for many-parallel-task computing (MPTC). JETS executes short-duration MPI tasks at scale using pilots managed by Coasters and workloads codified in the Swift scripting language. RP enables MPI executions natively, decoupling the implementation of application-side patterns of distributed computation like MPTC from the resource-side communication capabilities like MPI. JETS uses runtime features available in the MPICH MPI implementation [37], similar to RP using runtime features from OpenRTE [38], a component of the OpenMPI MPI implementation.

The implementation of pilots on HPC resources is particularly challenging when the $fork()/exec()$ call is not made available to the users as, for example, on the IBM BG/Q machines. This call is used to enable application-side scheduling of tasks on pilots executed on the resource compute nodes. Swift has circumvented this limitation by supporting the sub-jobs feature of the Cobalt scheduler [39], available for example on Mira, an IBM BG/Q at ALCF. RP generalizes this approach by directly using sub-jobs as supported by the IBM BG/Q operating system, avoiding the dependency on the Cobalt scheduler.

Swift/T, the latest incarnation of Swift [40] (T of Turbine [41]), steps away from the orchestration of executables by interpreting tasks as functions. This requires tasks to be codified as functions instead of executables, for example via the main-wrap technique presented in [39]. While promising in terms of performance, this approach creates obstacles for

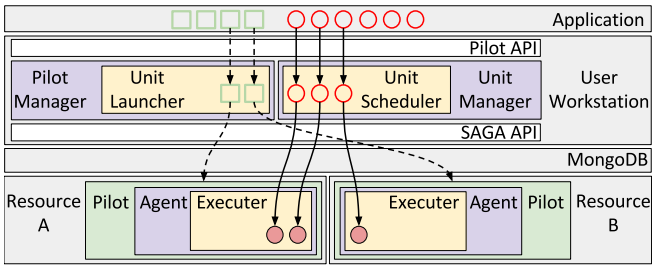

Figure 1: RP overview. An application uses the Pilot API to describe pilots (green squares) and units (red circles). The PilotManager instantiates (dash arrow) pilots, the UnitManager instantiates (solid arrow) units. Both managers are executed on the user workstation. Pilots are launched (dashed arrows) on resources A and B via SAGA API, an Agent is bootstrapped for each pilot, units are scheduled (solid arrow) to the Agents via MongoDB and executed by the Agent's Executer. Boxes color coding: gray for entities external to RP, white for APIs, purple for RP's modules, green for pilots, yellow for module's components.

both development and deployment of applications.

The Many-task computing [42] paradigm was introduced to bridge the gap between high throughput computing and high performance computing paradigms from a workload perspective. We make no presumptive constraints on workload duration, size or origin (e.g., distributed scientific workflows, multi-component applications).

III. Design and Architecture

RP is a runtime system designed to execute heterogeneous and dynamic workloads on diverse resources (Fig. 1). Workloads and pilots are described via the Pilot API and passed to the RP runtime system. RP launches the pilots and executes the tasks of the workload on them.

Internally, RP represents pilots as aggregates of resources independent from the architecture and topology of the target machines, and workloads as a set of units to be executed on the resources of the pilot. Both pilots and units are stateful entities, each with a well-defined state model and life cycle. Their states and state transitions are managed via the three modules of the RP architecture: PilotManager, UnitManager, and Agent (Fig. 1, purple boxes).

The PilotManager launches pilots on resources via the SAGA API. The SAGA API implements an adapter for each type of supported resource, exposing uniform methods for job and data management. The UnitManager schedules units to pilots for execution. A MongoDB database is used to communicate the workload between UnitManager and Agents. For this reason, the database instance needs to be accessible both from the user workstation and the target resources. The Agent bootstraps on a remote resource, pulls units from the MongoDB instance, and manages their execution on the cores held by the pilot.

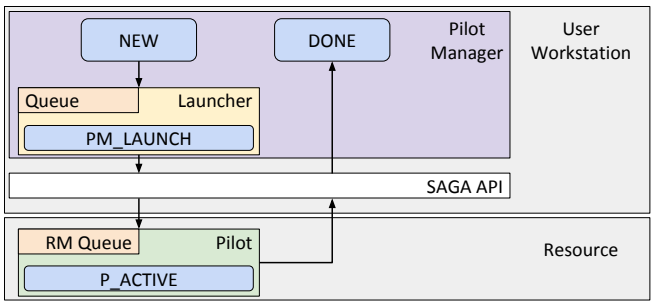

Figure 2: Pilot State Model. Instantiated in state NEW, each pilot is launched (PM_LAUNCH) via SAGA API on a resource manager. After becoming P_ACTIVE, it exhausts its duration ending in state DONE. The transition between states is sequential and each transition can be canceled or fail ending in the states CANCELED or FAILED (not depicted to improve the diagram clarity). Boxes color coding as per Fig. 1, with: orange for queues and blue for states.

A. State and Component Models

The lifespan of pilots has four states distributed among the PilotManager, resource, and pilot instance (Fig. 2). Pilots are instantiated in the state NEW by the PilotManager, wait in a queue to be launched, and transition to PM_LAUNCH when submitted to a Resource Manager (RM) via the SAGA API. Pilots wait in the queue of the RM and, once scheduled, become P_ACTIVE. They remain in this state until the end of their lifetime, when they transition to DONE.

The unit state model has nine states distributed across the UnitManager, MongoDB instance, and Agent (Fig. 3). Instantiated in the state NEW by the UnitManager, every unit is scheduled on an Agent (UM_SCHEDULING) via a queue on a MongoDB instance. The unit is then scheduled on the required number of cores held by the Agent's pilot (A_SCHEDULING), and finally executed (A_EXECUTING).

The unit state model pertains also to the input and output data of the units. When required, the input data of a unit are either pushed to the Agent (U_STAGING_IN) or pulled from the Agent (A_STAGING_IN), depending on data locality and sharing requirements. Similarly, the output data of the unit are staged out by the Agent and UnitManager (A_STAGING_OUT, U_STAGING_OUT) to a specified destination, e.g., the user workstation. Both input and output staging are optional, depending on the requirements of the units. The actual file transfers are enacted via SAGA, and support (gsi)scp, (gsi)sftp, and Globus Online.

The state transitions represented in Figures 2 and 3 are sequential and every transition can fail or be canceled by the PilotManager or UnitManager. All state transitions are managed by the PilotManager, UnitManager, and Agent components. The only special case is the transition of the pilots to the state P_ACTIVE which is dictated by the resource's RM, but managed by the PilotManager.

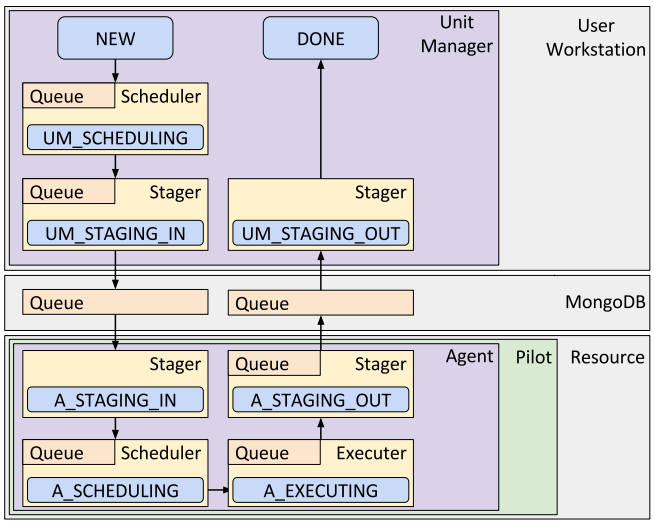

Figure 3: Unit State Model. Instantiated in state `NEW`, each unit is scheduled to an Agent (`UM_SCHEDULING`) via MongoDB, and then scheduled to an Agent's Executer (`A_SCHEDULING`). When required, unit input data are staged to the Agent's Pilot (`UM_STAGING_IN` or `A_STAGING_IN`). Each unit is executed (`A_EXECUTING`), unit output data are staged out (`A_STAGING_OUT` and `UM_STAGING_OUT`), and each unit ends in state (`DONE`). Color coding and state omissions as per Fig. 2.

Each component of RP has a independent semantic scope. This enables modularity isolating implementation complexity and supporting diverse use cases and environments. For example, unit scheduling can be implemented by exchangeable Scheduler components, suitable for applications of diverse scales, with different coordination patterns, and executed on Beowulf clusters or Cray machines.

Components are also designed to be stateless and instantiated concurrently. In this way, RP can manage multiple pilots and units at the same time, resulting in scalable throughput and tolerance to failing components. Concurrent components are coordinated via a dedicated communication mesh which incurs infrastructure and runtime overhead, offset by the lower component complexity and improved overall scalability of the system.

B. RP Modules

The modules of RP are distributed between the user workstation and the target resources. The PilotManager and UnitManager are executed on the user workstation while the Agent runs on the target resources. RP requires Linux or OS X with Python 2.7 or newer on the workstation but the Agent has to execute different types of units on resources with very diverse architectures and software environments.

RP manages these heterogeneities via the Launcher component of the PilotManager (Fig. 2), and the Stager, Scheduler and Executer components of the Agent (Fig. 3). The Launcher uses resource configuration files to define the number, placement, and properties of the Agent's components of each Pilot. Configuration files are made available for resources of XSEDE, NCSA, NERSC, ORNL but users can provide new files or alter existing configuration parameters at runtime, both for a single pilot or a whole RP session.

Depending on the architecture of the resource, the Agent's Stager, Scheduler, and Executer components (Fig. 3) can be placed on cluster head nodes, MOM nodes, compute nodes, virtual machines, or any combination thereof. Multiple instances of the Stager and Executer component can coexist in a single Agent, placed on any service node or compute node of the pilot's allocation. ZeroMQ communication bridges connect the Agent components, creating a network to support the transitions of the units through components.

Once instantiated, each Agent's Scheduler gathers information from the RM, retrieving the number of cores held by the pilot on which the Agent is running and how those cores are partitioned across nodes. Currently, the Scheduler acquires information from physical or virtual Linux machines and the following RMs: TORQUE, PBS Pro, SLURM, SGE, LSF, LoadLeveler, and Cray CCM.

Depending on requirements, the Agent's Scheduler assigns cores from on one or more nodes to each unit, setting the cores to "BUSY". For example, cores on a single node are assigned to multithreaded units while, cores on topologically close nodes are assigned to MPI units to minimize communication overheads. Two scheduling algorithms are currently supported: "Continuous" for cores organized as a continuum, and "Torus" for cores organized in an n-dimensional torus, as found, for example, on IBM BG/Q.

The Agent's Scheduler passes the units on to one of the Agent's Executers and Executers use resource configuration parameters to derive the launching command of each unit. Currently, RP supports the following launching methods: MPIRUN, MPIEXEC, APRUN, CCMRUN, RUNJOB, DPLACE, IBRUN, ORTE, RSH, SSH, POE, and FORK. Each resource is configured with two launching methods, one for MPI tasks and one for serial tasks.

Agent's Executers execute units via one of the two launching methods depending on the unit parameters and on the characteristics of the execution environment. Two spawning mechanisms are available: "Popen", based on Python, and "Shell", based on `/bin/sh`. Executers monitor the execution of the units, collect exit codes, and communicate the freed cores as "FREE" to the Agent's Scheduler.

C. Trade-offs

The design of RP supports heterogeneous and dynamic workloads and resources. As seen in §III-A and §III-B, heterogeneity is supported by implementing interoperability at multiple levels. The Pilot API enables the description of generic workloads, the SAGA API abstracts the specificity

of resource interfaces and RMs while the Scheduler and Executer of the Agent support multiple scheduling, launching, and process spawning methods. As a result, scalar, MPI, OpenMP, multi-process, and multi-threading units can be executed with shared or non-shared input data.

Workload and resource dynamism are supported by implementing modularity and executing multiple instances of each module. The modules and components of RP are stateless, pluggable, and can be transparently exchanged. Multiple instances of UnitManager and PilotManager can manage various pilots, bootstrapping several Agents on many resources. Multiple Agent's Stager, Executer, (and soon) Scheduler components can be concurrently instantiated, supporting the execution of many workloads on a varying number of pilots and resources.

The distributed, modular, and concurrent design of RP introduces complexities with both usability and performance overheads. RP however improves usability both at application and resource level by offering: a unified configuration system with default support for multiple HPC and HTC resources; user-level execution with no services installed or configured on target resources; and templates and coding facilities to develop modules supporting new resources, scheduling algorithms, and launching methods.

The performance overheads of RP's design require experimental characterization as they depend on the properties of both the workloads and the resources used for the execution. The execution overheads introduced at resource level are particularly relevant as they affect the execution of every unit, independent of whether the workload is divided in stages, or bounded by task dependences. The overheads introduced by bootstrapping the components of the Agent, scheduling the units, and launching them contribute to the overall time to completion of the workload.

IV. Performance Characterization

We use two metrics to characterize the performance of RP: total time to completion (TTC) of the given workload and resource utilization (RU). TTC is a measure of how fast an application can be executed on RP; RU a measure of the percentage of available resources used by the execution. Both metrics are relevant for HPC resources, which traditionally have been designed and operated so as to maximize overall utilization.

The execution of workloads comprised of many, possibly heterogeneous and dynamic tasks require the interplay of all RP's components and their supporting infrastructures. Nonetheless, as seen in §III, Figures 1-3, RP reduces every workload down to the execution of a set of units on one or more independent Agents. Once retrieved by an Agent, the execution of the units is performed in isolation, on the resources of the Agent's pilot. As such, the characterization of TTC and RU depends on how each individual component of the Agent and the Agent as a whole perform.

The following experiments search the parameter space of the Agent performance at both the component and module level. At the component level, each Agent's component is stress-tested in isolation measuring its theoretical maximum performance when managing an increasing number of units. At module level, the Agent is tested by executing a synthetic workload and measuring the Agent's subset of TTC and the RU of the pilot's resources on which the workload is executed.

We use a synthetic single-core workload for the module level experiments, varying the duration of each unit. This is the only parameter of the workload that affects the performance of the Agent and its components as the Agent handles execution of all types of units, single or multi-core, analogously. All units are scheduled on the pilot's resources by the Agent's Scheduler component via the Continuous or Torus scheduling algorithm, and spawned and launched by the Agent's Executor via the Popen or shell-based mechanism. Specifically, n-core units impose roughly $1/n$ times the scheduling overhead, $1/n$ times the execution overhead, and $1/n$ times the staging overhead, per core, compared to single-core units. As such, execution of multiple 1-core units represent the worse case scenario and the type of workload that can be best used to stress the Agent performance.

The performance of each Agent's module is bounded by that of the pilot's resources as, for example, spawning depends on creating processes on the node's operating system or communication and coordination via the nodes internal network. Thus, we perform experiments on three HPC resources, which are representative of the range and type of resources available to the computational science community: (i) ***Comet*:** a 2 PFLOP cluster at SDSC, with 24 Haswell cores 128GB RAM per node (6,400 nodes), Infiniband, Lustre shared filesystem (FS); (ii) ***Stampede*:** a 10 PFLOP cluster at TACC, with 16 Sandy Bridge cores / 32GB RAM per node (1,944 nodes), Infiniband, Lustre shared FS; and (iii) ***Blue Waters*** a 13.3 petaFLOPS Cray at NCSA, with 32 Interlago cores / 50GB RAM per node (26,864 nodes), Cray Gemini, Lustre shared FS.

RP is instrumented with a profiling facility to record timestamps of its operations. The recorded events are written to disk and utility methods are used to fetch and analyze them. RP's profiling is designed to be non-invasive and have minimal effect on the runtime. We measured the temporal overhead of the profiler by running a benchmark we developed to test RP overall performance. For the same workload executed on the same resources, the benchmark measured $144.7 \pm 19.2s$ with profiling, and $157.1 \pm 8.3s$ without. Note how the standard deviation of the two measurements overlap making the difference between the two execution times statistically insignificant.

A. Performance Metrics and Overheads

We use three performance metrics directly related to TTC and RU: number of units handled per second, a subset of TTC, and core utilization. The experiments at component level characterize the performance of each Agent's component in isolation by measuring the (time-variant) rate at which the individual components can handle units (in $units/second$). The experiments at module level characterize the aggregate performance of the Agent by measuring temporal efficiency as the subset ttc_a of TTC, and spatial efficiency as core utilization over ttc_a.

ttc_a is the time spent by the Agent to manage and execute units. ttc_a spans between the first units entering `A_STAGING_IN` state, and the last unit leaving `A_STAGING_OUT` state (Fig. 3). In this way, ttc_a isolates the elements of TTC that depend exclusively on RP's Agent.

Core Utilization is the percentage of cores used during ttc_a, integrated over time. It is thus a function of how many units are in the `A_EXECUTING` state at any point in time of ttc_a (Fig. 3). Ideally, the Agent would be able to immediately use all cores, keep all cores busy until all units are done, and then immediately free all cores, which would result in the ideal utilization of 100%.

B. Micro-benchmarks

Micro-benchmarks measure the performance of individual RP components *in isolation*. In a micro-benchmark, RP launches a Pilot on a resource with a single Unit scheduled to the Agent. When the Unit enters the component under investigation, it is cloned a specified number of times (10,000 times in our experiments). All the clones are then operated on by the component and dropped once the component has terminated its activity. This ensures that the downstream components remain idle. The result is that single components can be stressed in isolation, with a realistic workload, and without the influence of any other components. This approach to micro-benchmarks has two side effects: RP components and communication channels do not compete for shared system resources and, the benchmarked component cannot be affected by bottlenecks in other components. Thus, the micro-benchmark measures the *upper bound* of component performance, as reached *in isolation* from the interactions with other components.

We perform micro-benchmarks for three Agent components: the Scheduler, Stager and Executer. Results for both the input and output Stagers are discussed together, as both components behave analogously. We measure the performance of these components for three resources (*Stampede*, *Blue Waters* and *Comet*), and for several load-sharing setups (1, 2, 4, 8, 16, 32 component instances; distributed over 1, 2, 4, 8 compute nodes). These configurations span a large parameter space for the experiment, thus it is not possible to present the full set of results. We focus on those which most clearly illustrate the overall behavior of RP, in the sense that they expose performance and scaling differences between component types. The full set of profiling data and plots is available at [43].

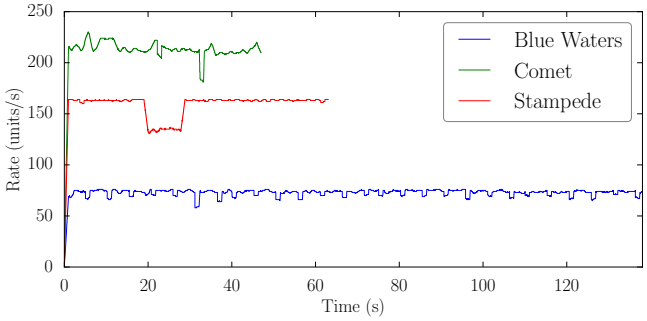

Figure 4: Performance of the Agent's Scheduler component. Measured as throughput, i.e., rate of units assigned to free cores per second, including both core allocation and de-allocation. Stable over time but different across resources.

Our experiments based on micro-benchmarks investigate: how quickly the Scheduler, Stager and Executor reach steady throughput, and the value of the steady-state throughput as a function of the number of component instances and their distribution.

1) Agent Scheduler Performance: Currently, RP can instantiate exactly one Scheduler component per Agent. The Scheduler is compute and communication bound: the algorithm searches repeatedly through the list of managed cores; core allocation and de-allocation are handled in separate, message driven threads. Fig. 4 shows how the component performs on three resources: the scheduler throughput stabilizes very quickly in all three cases, but the absolute values differ significantly (*Blue Waters*: $[72 \pm 5]/s$, *Comet*: $[211 \pm 19]/s$, *Stampede*: $[158 \pm 15]/s$), presumably due to differences in the resource's system performance (the RP configurations are identical).

2) Agent Output Stager Performance: The Agent output Stager is expected to be constrained by the read performance of the FS. Our experiments exclude actual file transfers, the activity of the component reduces to read very small `stdout` and `stderr` files from the FS, thus mostly stressing the FS' metadata management capabilities.

Fig. 5(a) shows the performance of one component instance on the three resources. We observe very little jitter, and relatively high unit throughput for all three machines: (*Blue Waters*: $[492s \pm 72]/s$, *Comet*: $[994s \pm 189]/s$, *Stampede*: $[771s \pm 128]/s$). We assume that the observed high throughput is due to FS caching, which usually is very efficient for Read operations. Consistently, the throughput of the input Stager, which in our experiments also stresses the FS' metadata management, performs at a throughput of about 1/3rd (no plot shown), with significantly larger jitter,

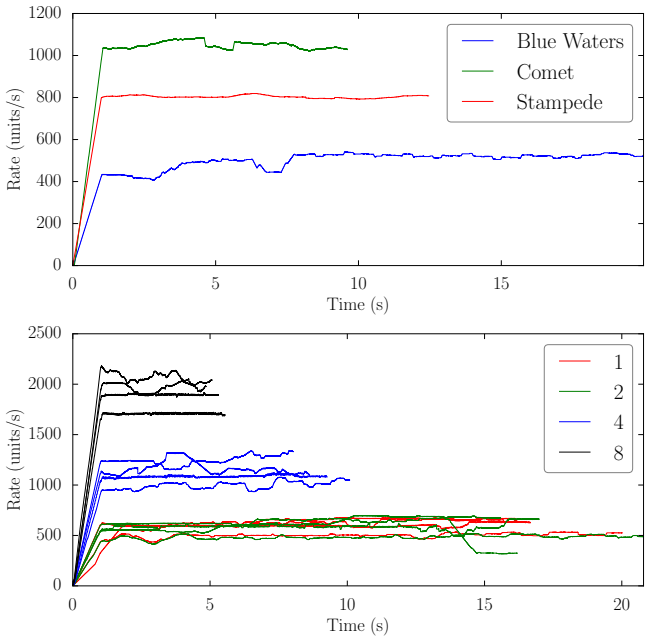

Figure 5: **(top)** Performance of the Agent's output Stager component. Measured as the rate of units handled per second. 1 Stager, 1 node: rate is stable over time but different across resources due to FS performance. **(bottom)** Combinations of 1,2,4 Stagers on 1,2,4,8 *Blue Waters* nodes: rate reflects an architecture with two nodes sharing a network router. Rate only improves when Stagers are spread over multiples of two nodes, independent of the actual number of Stagers (different lines in the same color show different numbers of Stagers per node).

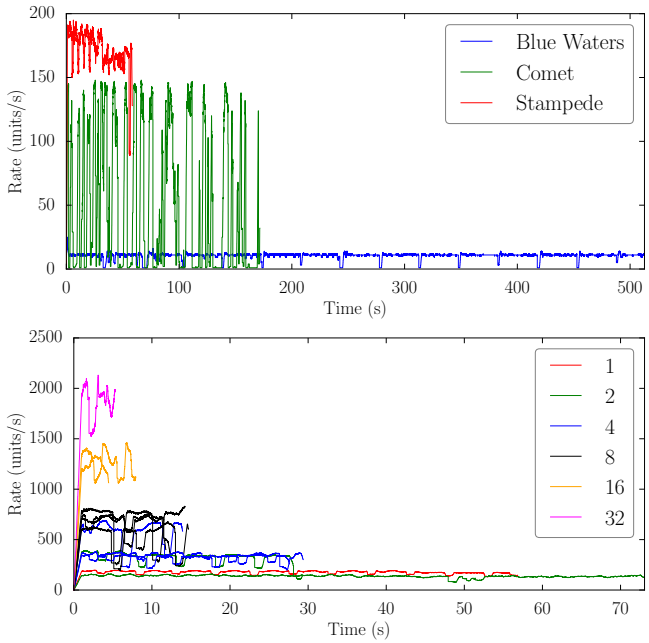

Figure 6: **(top)** Performance of the Agent's Executor component. Measured as the rate of units handled per second. 1 Stager, 1 node: rate varies over the resources – both in jitter and absolute values. **(bottom)** Combinations of 1,2,4 Executers on 1,2,4,8 *Stampede* nodes: rate improves for multiple Executers, independent of their distribution over nodes (lines of the same color show the same total number of instances in different node distributions).

reflecting the fundamental limitations of write caching in shared file systems.

Fig. 5(b) plots the scaling behavior on *Blue Waters* when varying the number of component instances and their distribution over compute nodes. On one and two nodes, the throughput does not vary significantly, and does not depend on the total number of components used ($[490...526 \pm 63...120]/s$). When using 4 or 8 nodes, we do observe a good scaling of throughput ($4 : [948...1168 \pm 178...245]/s$, $8 : [1552...1851 \pm 390...500]/s$), indicating that the shared FS is able to load-balance among compute nodes. The performance of metadata operations on Lustre FS is specified to about 1,000/s metadata operations per client[44]. Assuming that such operations are mostly communication bound, the observed behavior can be explained by the *Blue Waters* architecture: two nodes share a single Gemini router [45], so RP only scale in throughput when using multiples of 2 nodes, as evident in figure 5(b).

3) Unit Execution Performance: The process of spawning and managing application tasks is central to the Agent's Executor component, and this is where the resources are observed to differ most significantly in their average throughput, jitter and scaling behavior. Fig. 6(a) shows the throughput 1 component instance: *Blue Waters* is observed to have a very consistent, but low rate of $[11 \pm 2]/s$ *Comet* shows an average rate of $[102 \pm 42]/s$, which though varies significantly over time. *Stampede* has a relatively high rate of $[171 \pm 20]/s$, with less jitter than *Comet*.

Fig. 6(b) shows the scaling behavior for *Stampede*: the throughput scales with both the number of nodes and the number of components per node. Specifically, the combination of 8 nodes with 2 Executors per node ($[1188 \pm 275]/s$) performs similar to the combination of 4 nodes with 4 Executors each ($[1104 \pm 319]/s$), suggesting that the scaling is independent of the component placement, and thus represents an RP implementation limit rather than a system limit. The 8 nodes times 4 components configuration achieves a throughout of $[1685 \pm 451]/s$ but at that point the jitter begins to increase compared to the smaller configurations, indicating increased stress on the node OS.

We also investigated the scaling of throughput over number and distribution of Executors on *Blue Waters* and *Comet* (no plots shown). For *Blue Waters*, the jitter increases very quickly, while the average throughput increases by up to a

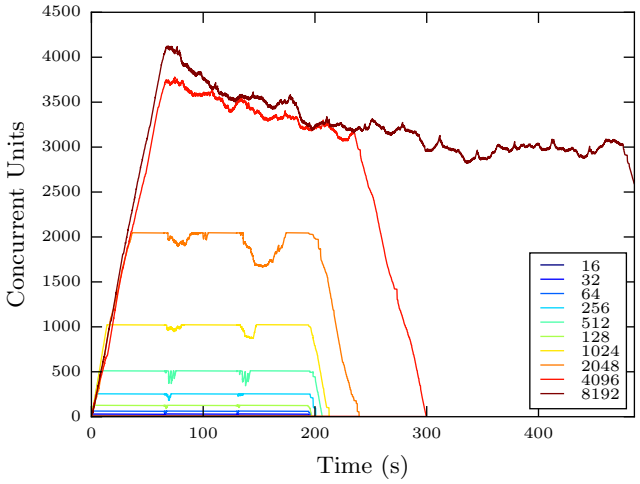

Figure 7: Observed unit concurrency as a function of pilot size on *Stampede*. The workload for each experiment is constrained to be three times the size of the Pilot. All units run for 64 seconds and are executed using the SSH launch method. The 4k and 8k runs do not reach their maximum for this unit duration.

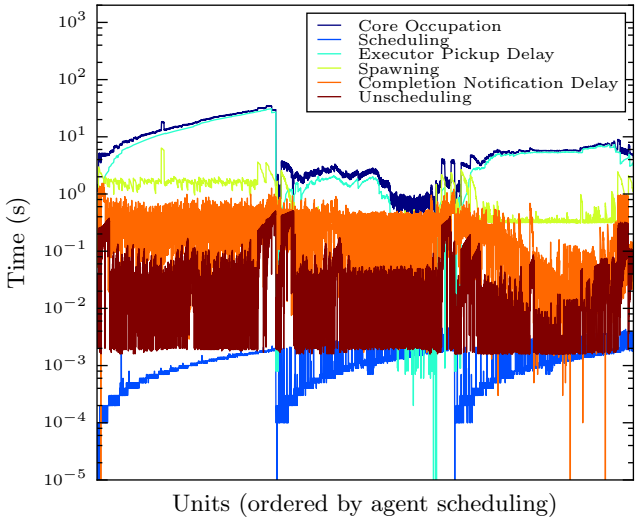

Figure 8: Decomposition of core occupation time for each unit. The workload consists of 6144 units of 64s on a 2048 core pilot on *Stampede* executed with the SSH launch method. "Core occupation" is the period RP has marked the pilot cores "BUSY" for the unit. The other measures are the chronological phases each unit spends time in.

factor of 2.5. *Comet*'s average throughput scales similarly to *Stampede*, but the observed jitter also increases further.

C. Agent Performance

To characterize the different aspects of agent performance we employ workloads that although simplified, capture the critical application requirements in Section I. The workloads have varying unit duration and are executed on pilots of different sizes. The size of each unit is set to one core; from a functional and performance perspective of RP the size of a unit is not relevant. Setting each unit to be a single core permits experiments that stress RP the fullest extent possible for a given Pilot size.

It is often the case that there are more tasks than can be run concurrently. We then use the term *generation* to describe a subset of the total workload, that fits concurrently on the cores held by the pilot. For example, if we have 48 tasks of a single core that need to be executed on a 16 core Pilot, there will be three generations of units. If each task is 60 seconds in duration, the optimal ttc_a would be 180 seconds (3 generations $\times$ 60 seconds).

In principle, the upper bound of agent performance is the performance of its slowest component but, in practice, the Agent performance can be lower due to at least three reasons: (i) the micro-benchmarks neglect the influence of communication between components; (ii) the concurrent operation of multiple components introduces competition for shared system resources (e.g., both input and output staging compete for FS resources); and (iii) the Agent performance can be limited by slower RP components or system resources *outside* of the agent scope.

The set of agent-level experiments discussed in this Subsection investigate the contributions of (i) and (ii). To offset (iii), we design experiments so that the agent operates in isolation, i.e., it is independent of the performance of the PilotManager and UnitManager and their interaction with the agent. Specifically, we ensure that the agent receives sufficient work to fully utilize the pilot's resources, by introducing a startup barrier in the agent ensuring that it only starts to process units once the complete workload has arrived at the agent.

In Fig. 7 we analyse RP's ability to fill all available cores with Units on *Stampede*. We fix the duration of the units to 64s and vary the number of cores available to the pilot. The workload for each experiment is comprised of 3 generations of units. On the y-axis we can see resulting number of units running concurrently and on the x-axis the ttc_a of the respective workload as a result of that. The optimal ttc_a would be 192 seconds for all runs.

The initial slope represents the rate of unit launch, which is are similar for all runs. As a consequence of the launch rate in relation to the unit duration and number of cores, the number of concurrent units reaches a ceiling of around 4100 for this set of experiments. Thus, the pilot of 4k cores is barely fully utilized and the 8k pilot underutilized. The concurrency ceiling has the same effect on both the 4k and 8k runs, with the only difference that the 8k therefore needs longer to complete.

Fig. 8 shows for each unit, the time spent from "Scheduling" onto a core (A_SCHEDULING) until

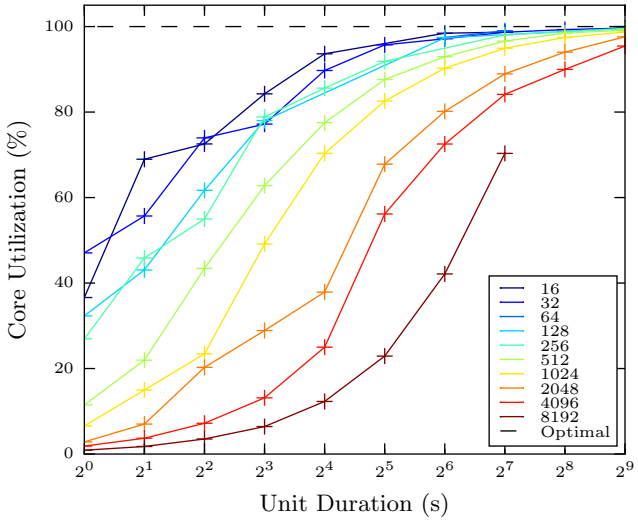

Figure 9: Core utilization as a function of task runtimes and pilot sizes. The workload for every experiment consists of three times the number of units than that would fit concurrently on the pilot. Results shown for *Stampede* with the SSH launch method.

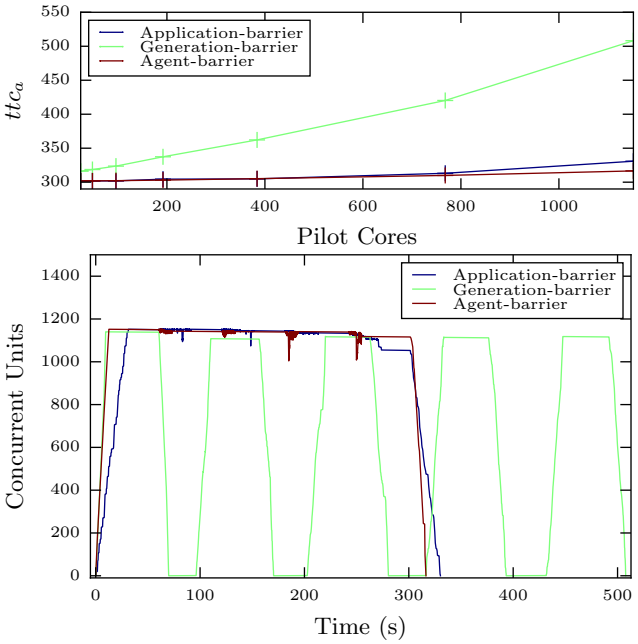

Figure 10: **(top)** ttc_a of workloads with different barrier types. The workloads for every run consists of five generations on a varying number of cores (24, 48, 96, 192, 386, 768, 1152). **(bottom)** Unit concurrency for the three barrier types for a 1152 core pilot executing 5760 units. See text for description of different barriers.

the "Unscheduling" where the core is released (A_STAGING_OUT_PENDING). The data represents the 2048 core run from Fig 7. We can distinguish the 3 generations, most clearly from the shape of the scheduling trace in blue. Although scheduling is relatively quick for all units, we see an increase within a generation, which is explained by the linear list operation in the scheduling algorithm. The scheduler assigns a core to the unit, which makes it eligible to be picked up by the executer (A_EXECUTING_PENDING). The "Core Occupation Overhead" is the time RP has a core marked "BUSY" for a unit minus the actual runtime of the unit (between the unit enters the A_SCHEDULING state and leaves the A_EXECUTING state). The largest contributing factor to core occupation overhead is the time it takes from core assignment (A_EXECUTING_PENDING) until actual launch by the executer (A_EXECUTING). The slope of the "Executor Pickup Delay" relates to the rate of execution from Fig 7, in that all units of the first generation are assigned a core almost immediately by the scheduler, but that it takes time until the last unit of the first generation is launched by the executer. The spawning overhead during the first generation is (slightly) higher than for subsequent generations, which is explained by the fact that for the consecutive generations the spawning is more gradual, and therefore suffers less from contention.

To build intuition into the efficiency of running a certain workload, we investigate the effect of the unit runtimes on the core utilization. The results for *Stampede* are in Fig. 9. For short unit durations, the overhead of the launch rate is relatively high, resulting in lower utilization rate at higher core counts. For longer running units the impact of the launch rate decreases, first for smaller core counts then for larger ones.

D. Integrated Performance

The following experiments are designed to evaluate the response of RP to an end-user application. They examine different workload barriers which represent what end-user applications encounter. Most importantly this factors in the communication between UnitManager and agent that we excluded until now. The workload for each experiment is consists of 5 generations of single core units and the duration of each Unit is 60s.

In the first scenario we re-use the configuration from the Agent-level experiments, i.e., the entire workload is available at the start of the Agent ("Agent-barrier"). In the second scenario, that order is reversed, i.e., the Agent is started first and then the UnitManager starts to feed the workload to the Agent ("Application-barrier"). In the third scenario, the application creates a barrier after every generation, and it does not start to feed next-generation Units to the Agent until all Units of the previous generation are completed ("Generation-barrier"). The optimal TTC for this workload is 300 seconds.

Fig. 10 (top) shows that the performance difference between the Agent-barrier and Application-barrier are negligible for small core counts, but become noticeable when the Pilot has more than 1k cores. In Fig. 10 (bottom) we focus on the experiment conducted with 1152 cores and we see that the offset is primarily caused by the different unit startup rates. This is explained by the fact that in the Agent-barrier scenario all workload is ready to run at the Agent side while in the Application-barrier scenario the workload still needs to be communicated to the Agent. The performance of the Generation-barrier shows considerable overhead for experiments at smaller core counts. The detailed plot in Fig. 10 (bottom) shows prolonged periods of core idleness between the generations. During this period the status of the units are communicated back to the UnitManager, and the workload of the next generation is submitted to the Agent; the communication delay causes core idleness. The communication load increases with the number of units, and thus with the number of cores, which explains the growth of the overhead with increasing core counts. The execution rate of the Generation-barrier run for consecutive generations is consistent with that of the Application-barrier.

V. Discussion

We started with micro-benchmarks which offer insight on how each individual Agent component performs on diverse target resources for different Agent configurations (Sec. IV-B). These benchmarks provided an upper-bound on the performance of each component showing system specific dependences. Unexpectedly, the Agent's Scheduler performance pointed towards differences in Python execution efficiency (Fig. 4) while subtle architecture dependences emerged in the performance of multiple instances of the Agent's Stager (Fig. 5). Interestingly, the number of Executer instances per node was shown to be irrelevant for unit execution performance, up to the scale tested (Fig. 6).

We then performed Agent-level benchmarks, executing heterogeneous workloads on heterogeneous pilots with different Agent's configurations. This characterized the aggregated performance of the Agent's components, confirming that it is mostly a composition of the individual components' performance, supporting the architectural choices of RP. Accordingly, the Agent's Executer was the slowest component of the Agent, primarily due to unit spawning overhead (Fig. 8). This confirmed the performance bound of the system and Python process management as observed with the micro-benchmarks, especially when executing multiple generations within the same pilot. Scalability across pilot size is instead confirmed, suggesting that performance will be stable for increasingly larger pilots and a single generation execution (Fig. 7).

The primary objective of RP's design is to support heterogeneity and dynamism both for workloads and resources. Our experiments show how RP is used on heterogeneous resources with differing architectures and software environment. They also show how RP does not place constraints on the size and duration of the units, enabling variation of these parameters at unit level and across workload generations. As such, these experiments validate the primary design decisions while characterizing RP's performance and establishing limits to its scalability.

Our experiments show that performance increases with the increase of units duration. The concurrent execution of short units increases the overlap between their spawning and running phases. For similar reasons, there is a degradation when executing multiple workload generations on the same pilot. Importantly, the rate at which these performance limitations affect heterogeneity and dynamism is mostly independent of the size of the pilot. The rate depends instead on the ratio between the number of tasks in a workload and the number of cores available on the pilot. As Unit size is the smallest possible, the performance results represent a lower-bound: for the same number of units, utilization improves as the size of the Unit increases.

VI. Conclusion

Prima facie, a system implementing the Pilot abstraction [10, 11] provides the conceptual and functional capabilities needed to support the scalable execution of dynamic and heterogeneous workloads. The impact of an abstraction is limited to its best implementation. Whereas there are multiple pilot systems, they are either geared towards specific functionality or platforms. Against this backdrop, RADICAL-Pilot (RP) brings together recent conceptual advances [10, 11] with advances in systems & software engineering, and open source and community best practices.

This paper describes the architecture and implementation of RP (Sec. III), and characterizes the performance of its Agent module on three HPC platforms (Sec. IV). RP is a system that is: (i) adaptable to a wide variety of requirements in terms of heterogeneity of workloads and resources, (ii) amenable to abstract performance analysis and optimization, and (iii) currently has performance that is resource-limited and not implementation or design limited (Sec.V).

Given the diversity of current [46] and future workloads that will utilize HPC systems (see Ref. [47] for a recent analysis on NERSC systems), the scalable execution of dynamic and heterogeneous workloads is a critical requirement. For the domain of molecular sciences, there is a demonstrated need [48] to be able to support up to 10^5 MPI tasks as part of a single "simulation".

RP will need to be re-engineered to efficiently execute workloads at this scale. Immediate improvements can be obtained by modifying the interaction among RP's modules and to avoid exposing resource limitations. However, most of the benefits will come from improving the Agent, consistently with what argued and shown in §III and §IV. We are planning to: (i) Develop a concurrent Scheduler

to support partitioning of the pilot resources and having multiple agents operating in parallel on these partitions; (ii) Explore new launch methods developing and experimenting new Executer implementations; and (iii) aggregating units depending on their application provenance and duration to optimize throughput.

The focus of this paper has been on the direct execution of workloads on HPC machines, but RP also forms the middleware system for a range of high-performance application-tools [49–52], already use in production. RP also serves a vehicle for research in distributed [53] and data-intensive scientific computing [54]. RP is available for immediate use on many contemporary platforms [55]. RP source is accompanied with extensive documentation and an active developer-user community.

ACKNOWLEDGEMENTS

This work is supported by NSF "CAREER" ACI-1253644, NSF ACI-1440677 "RADICAL-Cybertools" and DOE Award de-sc0008651. We acknowledge access to computational facilities on XSEDE resources via TG-MCB090174, and support of NSF-1516469 which provides access to NSF's Blue Waters. We thank members of the RADICAL group for useful comments, feedback and testing.

AUTHOR CONTRIBUTION

Andre Merzky is the lead developer of RADICAL Pilot, designed/performed the micro-benchmark experiments. Mark Santcroos is senior developer of RADICAL Pilot, is responsible for the implementation and optimization of the Agent abstraction layers and job spawning mechanisms. He designed and executed the Agent-level and Integrated experiments. Matteo Turilli has played an important role in the testing and design discussions of RADICAL Pilot, and in writing of this paper. Shantenu Jha is the project lead.

REFERENCES

[1] J. Preto and C. Clementi, "Fast recovery of free energy landscapes via diffusion-map-directed molecular dynamics," *Physical Chemistry Chemical Physics*, vol. 16, no. 36, pp. 19 181–19 191, 2014.

[2] T. E. Cheatham III and D. R. Roe, "The impact of heterogeneous computing on workflows for biomolecular simulation and analysis," *Computing in Science & Engineering*, vol. 17, no. 2, pp. 30–39, 2015.

[3] Y. Sugita and Y. Okamoto, "Replica-exchange molecular dynamics method for protein folding," *Chemical physics letters*, vol. 314, no. 1, pp. 141–151, 1999.

[4] B. Austin, T. Butler, R. Gerber, C. Whitney, N. Wright, W.-S. Yang, and Z. Zhao, *Hopper Workload Analysis*, May 2014. [Online]. Available: http://www.osti.gov/scitech/servlets/purl/1163230

[5] T. R. Furlani, B. L. Schneider, M. D. Jones, J. Towns, D. L. Hart, S. M. Gallo, R. L. DeLeon, C.-D. Lu, A. Ghadersohi, R. J. Gentner, A. K. Patra, G. von Laszewski, F. Wang, J. T. Palmer, and N. Simakov, "Using XDMoD to facilitate XSEDE operations, planning and analysis," in *Proceedings of the Conference on Extreme Science and Engineering Discovery Environment: Gateway to Discovery*, ser. XSEDE '13. New York, NY, USA: ACM, 2013, pp. 46:1–46:8. [Online]. Available: http://doi.acm.org/10.1145/2484762.2484763

[6] Singhal, N., & Pande, V. S. (2005). Error analysis and efficient sampling in Markovian state models for molecular dynamics. The Journal of chemical physics, 123(20), 204909.

[7] Pronk, S., Larsson, P., Pouya, I., Bowman, G. R., Haque, I. S., Beauchamp, K., ... & Lindahl, E. (2011, November). Copernicus: A new paradigm for parallel adaptive molecular dynamics. In Proceedings of 2011 International Conference for High Performance Computing, Networking, Storage and Analysis (p. 60). ACM.

[8] Noe, F., Schaijtte, C., Vanden-Eijnden, E., Reich, L., & Weikl, T. R. (2009). Constructing the equilibrium ensemble of folding pathways from short off-equilibrium simulations. Proceedings of the National Academy of Sciences, 106(45), 19011-19016.

[9] E. Hwang, S. Kim, T. k. Yoo, J. S. Kim, S. Hwang, and Y. r. Choi, "Resource allocation policies for loosely coupled applications in heterogeneous computing systems," *IEEE Transactions on Parallel and Distributed Systems*, vol. PP, no. 99, pp. 1–1, 2015.

[10] M. Turilli, M. Santcroos, and S. Jha, "A comprehensive perspective on pilot-jobs," 2016, (under review) http://arxiv.org/abs/1508.04180.

[11] A. Luckow, M. Santcroos, A. Merzky, O. Weidner, P. Mantha, and S. Jha, "P*: A model of pilot-

abstractions," *IEEE 8th International Conference on e-Science*, pp. 1–10, 2012, http://dx.doi.org/10.1109/eScience.2012.6404423.

[12] Pilot API, 2015, http://radicalpilot.readthedocs.org/.

[13] A. Merzky, O. Weidner, and S. Jha, "SAGA: A standardized access layer to heterogeneous distributed computing infrastructure," *Software-X*, 2015, dOI: 10.1016/j.softx.2015.03.001. [Online]. Available: http://dx.doi.org/10.1016/j.softx.2015.03.001

[14] A. Treikalis, A. Merzky, D. York, and S. Jha, "RepEx: A flexible framework for scalable replica exchange molecular dynamics simulations," 2016, (under review) http://arxiv.org/abs/1601.05439.

[15] V. Balasubramanian, A. Trekalis, O. Weidner, and S. Jha, "Ensemble toolkit: Scalable and flexible execution of ensembles of tasks," 2016, (under review) http://arxiv.org/abs/1602.00678.

[16] M. Wilde, M. Hategan, J. M. Wozniak, B. Clifford, D. S. Katz, and I. Foster, "Swift: A language for distributed parallel scripting," *Parallel Computing*, vol. 37, no. 9, pp. 633–652, 2011.

[17] T. Maeno, K. De, A. Klimentov, P. Nilsson, D. Oleynik, S. Panitkin, A. Petrosyan, J. Schovancova, A. Vaniachine, T. Wenaus *et al.*, "Evolution of the ATLAS PanDA workload management system for exascale computational science," in *Proceedings of the 20th International Conference on Computing in High Energy and Nuclear Physics (CHEP2013), Journal of Physics: Conference Series*, vol. 513(3). IOP Publishing, 2014, p. 032062.

[18] F. Berman, R. Wolski, S. Figueira, J. Schopf, and G. Shao, "Application-level scheduling on distributed heterogeneous networks," in *Proceedings of the ACM/IEEE Conference on Supercomputing*. IEEE, 1996, pp. 39–39.

[19] D. Thain, T. Tannenbaum, and M. Livny, "Distributed computing in practice: The Condor experience," *Concurrency and Computation: Practice and Experience*, vol. 17, no. 2-4, pp. 323–356, 2005.

[20] J. Frey, T. Tannenbaum, M. Livny, I. Foster, and S. Tuecke, "Condor-G: A computation management agent for multi-institutional grids," *Cluster Computing*, vol. 5, no. 3, pp. 237–246, 2002.

[21] J. T. Mościcki, "DIANE - distributed analysis environment for GRID-enabled simulation and analysis of physics data," in *Proceedings of the IEEE Nuclear Science Symposium Conference Record*, vol. 3. IEEE, 2003, pp. 1617–1620.

[22] P. Saiz, L. Aphecetche, P. Bunčić, R. Piskač, J.-E. Revsbech, V. Šego, A. Collaboration *et al.*, "AliEn: ALICE environment on the GRID," *Nuclear Instruments and Methods in Physics Research Section A: Accelerators, Spectrometers, Detectors and Associated Equipment*, vol. 502, no. 2, pp. 437–440, 2003.

[23] A. Casajus, R. Graciani, S. Paterson, A. Tsaregorodtsev *et al.*, "DIRAC pilot framework and the DIRAC Workload Management System," in *Proceedings of the 17th International Conference on Computing in High Energy and Nuclear Physics (CHEP09), Journal of Physics: Conference Series*, vol. 219(6). IOP Publishing, 2010, p. 062049.

[24] I. Sfiligoi, D. C. Bradley, B. Holzman, P. Mhashilkar, S. Padhi, and F. Würthwein, "The pilot way to grid resources using glideinWMS," in *Proceedings of the World Congress on Computer Science and Information Engineering*, vol. 2. IEEE, 2009, pp. 428–432.

[25] R. Pordes *et al.*, "The Open Science Grid," *J. Phys.: Conf. Ser.*, vol. 78, no. 1, p. 012057, 2007.

[26] J. Gyllenhaal, T. Gamblin, A. Bertsch, and R. Musselman, "Enabling high job throughput for uncertainty quantification on BG/Q," ser. IBM HPC Systems Scientific Computing User Group (SCICOMP), 2014.

[27] J. Cope, M. Oberg, H. M. Tufo, T. Voran, and M. Woitaszek, "High throughput grid computing with an IBM Blue Gene/L," *2007 IEEE International Conference on Cluster Computing (CLUSTER)*, pp. 357–364, 2007.

[28] E. Deelman, K. Vahi, G. Juve, M. Rynge, S. Callaghan, P. J. Maechling, R. Mayani, W. Chen, R. F. da Silva, M. Livny *et al.*, "Pegasus, a workflow management system for science automation," *Future Generation Computer Systems*, vol. 46, pp. 17–35, 2015.

[29] E. Deelman, G. Singh, M.-H. Su, J. Blythe, Y. Gil, C. Kesselman, G. Mehta, K. Vahl, G. B. Berriman, J. Good, A. Laity, J. C. Jacob, and D. S. Katz, "Pegasus: A framework for mapping complex scientific workflows onto distributed systems," *Scientific Programming*, vol. 13, no. 3, pp. 219–237, 2005.

[30] M. Albrecht, P. Donnelly, P. Bui, and D. Thain, "Makeflow: A portable abstraction for data intensive computing on clusters, clouds, and grids," in *Proceedings of the 1st ACM SIGMOD Workshop on Scalable Workflow Execution Engines and Technologies*. ACM, 2012, p. 1.

[31] A. Jain, S. P. Ong, W. Chen, B. Medasani, X. Qu, M. Kocher, M. Brafman, G. Petretto, G.-M. Rignanese, G. Hautier *et al.*, "FireWorks: a dynamic workflow system designed for high-throughput applications," *Concurrency and Computation: Practice and Experience*, 2015.

[32] P. Bui, D. Rajan, B. Abdul-Wahid, J. Izaguirre, and D. Thain, "Work Queue + Python: A framework for scalable scientific ensemble applications," in *Workshop on Python for High Performance and Scientific Computing at SC11*, 2011.

[33] I. Raicu, Y. Zhao, C. Dumitrescu, I. Foster, and M. Wilde, "Falkon: a Fast and Light-weight tasK executiON framework," in *Proceedings of the 8th*

ACM/IEEE conference on Supercomputing. ACM, 2007, p. 43.

[34] M. Hategan, J. Wozniak, and K. Maheshwari, "Coasters: uniform resource provisioning and access for clouds and grids," in *Proceedings of the 4th IEEE International Conference on Utility and Cloud Computing (UCC)*. IEEE, 2011, pp. 114–121.

[35] M. Rynge, S. Callaghan, E. Deelman, G. Juve, G. Mehta, K. Vahi, and P. J. Maechling, "Enabling large-scale scientific workflows on petascale resources using MPI master/worker," in *XSEDE '12: Proceedings of the 1st Conference of the Extreme Science and Engineering Discovery Environment: Bridging from the eXtreme to the campus and beyond*, Jul. 2012.

[36] J. M. Wozniak, M. Wilde, and D. S. Katz, "JETS: Language and system support for many-parallel-task workflows," *Journal of Grid Computing*, 2013.

[37] "Mpich web site," http://www.mcs.anl.gov/research/projects/mpich2.

[38] R. H. Castain and J. M. Squyres, "Creating a transparent, distributed, and resilient computing environment: the OpenRTE project," *The Journal of Supercomputing*, vol. 42, no. 1, pp. 107–123, Oct. 2007.

[39] K. Maheshwari, J. M. Wozniak, T. G. Armstrong, D. S. Katz, T. A. Binkowski, X. Zhong, O. Heinonen, D. Karpeyev, and M. Wilde, "Porting ordinary applications to Blue Gene/Q supercomputers," in *2015 IEEE 11th International Conference on e-Science (e-Science)*. IEEE, Aug. 2015, pp. 420–428.

[40] J. M. Wozniak, T. G. Armstrong, M. Wilde, D. S. Katz, E. Lusk, and I. T. Foster, "Swift/T: Large-scale application composition via distributed-memory dataflow processing," in *Cluster, Cloud and Grid Computing (CCGrid), 2013 13th IEEE/ACM International Symposium on*. IEEE, 2013, pp. 95–102.

[41] J. M. Wozniak, T. G. Armstrong, K. Maheshwari, E. Lusk, D. S. Katz, M. Wilde, and I. T. Foster, "Turbine: A distributed-memory dataflow engine for high performance many-task applications," *Fundamenta Informaticae*, vol. 128, no. 3, pp. 337–366, 2013.

[42] I. Raicu, I. T. Foster, and Y. Zhao, "Many-task computing for grids and supercomputers," in *Proceedings of the Workshop on Many-Task Computing on Grids and Supercomputers (MTAGS)*. IEEE, 2008, pp. 1–11.

[43] "RP experiment repository for micro benchmarks," https://github.com/radical-experiments/rp-paper-2015-micro/.

[44] "Manual of the LUSTRE File System," http://wiki.old.lustre.org/manual/LustreManual20_HTML/UnderstandingLustre.html.

[45] Q. Koziol *et al.*, *High performance parallel I/O*. CRC Press, 2014, page 19, section 3.1.

[46] L. R. Jay Srinivasan, Richard Shane Canon, "My Cray can do that? Supporting Diverse Workloads on the Cray XE-6," ser. Cray User Group 2012, May 2012.

[47] G. P. Rodrigo Álvarez, P.-O. Östberg, E. Elmroth, K. Antypas, R. Gerber, and L. Ramakrishnan, "HPC system lifetime story: Workload characterization and evolutionary analyses on NERSC systems," in *Proceedings of the 24th International Symposium on High-Performance Parallel and Distributed Computing*, ser. HPDC '15. New York, NY, USA: ACM, 2015, pp. 57–60. [Online]. Available: http://doi.acm.org/10.1145/2749246.2749270

[48] Shantenu Jha and Peter M. Kasson, "High-level software frameworks to surmount the challenge of 100x scaling for biomolecul ar simulation science," White Paper submitted to NIH-NSF Request for Information (2015) http://www.nsf.gov/pubs/2016/nsf16008/nsf16008.jsp, http://dx.doi.org/10.5281/zenodo.44377.

[49] "ExTASY Project," http://www.extasy-project.org/.

[50] B. K. Radak, M. Romanus, T.-S. Lee, H. Chen, M. Huang, A. Treikalis, V. Balasubramanian, S. Jha, and D. M. York, "Characterization of the three-dimensional free energy manifold for the Uracil Ribonucleoside from asynchronous replica exchange simulations," *Journal of Chemical Theory and Computation*, vol. 11, no. 2, pp. 373–377, 2015, http://dx.doi.org/10.1021/ct500776j. [Online]. Available: http://dx.doi.org/10.1021/ct500776j

[51] "Replica-Exchange Framework," https://github.com/radical-cybertools/radical.repex.

[52] "SPIDAL Project," http://www.spidal.org/.

[53] M. Turilli, F. F. Liu, Z. Zhang, A. Merzky, M. Wilde, J. Weissman, D. S. Katz, and S. Jha, "Integrating abstractions to enhance the execution of distributed applications," in *Proceedings of 30th IEEE International Parallel and Distributed Processing Symposium (IPDPS)*, 2016, http://arxiv.org/abs/1504.04720.

[54] "SC15 tutorial: Data-intensive applications on HPC using Hadoop, Spark and RADICAL-Cybertools," https://github.com/radical-cybertools/supercomputing2015-tutorial/wiki.

[55] "RADICAL-Pilot Github Project," https://github.com/radical-cybertools/radical.pilot.